

# Wake properties characterisation of marine current turbines

F. Maganga <sup>1,2</sup>, G. Pinon <sup>2</sup>, G. Germain <sup>1,3</sup>, E. Rivoalen <sup>4</sup>

<sup>1</sup> IFREMER, Hydrodynamic & Metocean Service, F-62321 Boulogne-sur-Mer, France  
fabrice.maganga@ifremer.fr

<sup>2</sup> Univ Le Havre, LOMC, FRE 3102 CNRS, F-76600 Le Havre, France  
gregory.pinon@univ-lehavre.fr

<sup>3</sup> Univ Lille Nord de France, F-59000 Lille, France

<sup>4</sup> INSA de Rouen, LMR, F-76801 Saint-Etienne du Rouvray, France  
elie.rivoalen@insa-rouen.fr

## Abstract

The hydrodynamics of a three bladed horizontal axis turbine is investigated. The performance of a turbine of 0.7 m of diameter and its wake were obtained from experiments and numerical simulations. A six components load cells is used for thrust and hydrodynamic power measurements, and Laser Doppler Velocimetry technics for wake characterisation. A three-dimensional software, taking into account the non stationary evolution of the wake generated by turbine blades is developed. The flow is discretised with particles carrying vorticity, which are advected in a Lagrangian frame.

Both numerical and experimental power coefficient  $C_p$  and velocity maps were compared. Experiments and numerical data showed a satisfactory agreement in term of the shape of the wake and of  $C_p$ , whereas the turbine was only modelled as a rotor composed of three blades. The results showed that the maximum decay of the wake velocity deficit is obtained in the near wake and the extension of velocity deficit until 10 D downstream. These studies highlight the problems that can appear during the configuration of turbines in a farm. The main aim of this work is to understand how the wake decays downstream, in order to estimate the effects produced in the lee side of turbines and more generally on its close environment.

**Keywords:** Experimental trials, flume tank, hydrodynamic, marine current turbine, Vortex Method.

## 1. Introduction

The debate on the climate change and the environment protection has led the most industrialized countries to set targets of reduction of gas emissions with greenhouse effects of 50 % from here to 2050 and of production of electricity from non-polluting energy.

Thus, the marine current energy was identified like the one of most promising green energies taking into account its foresee ability [1].

However, the deployment of marine current energy converters raise questions about flow conditions effects, turbine wake interactions effects and especially their environmental impact [12]. Modifications of the overall flow patterns in the area of current energy devices may alter the erosion and sediment transport by their wakes effects, and even the free surface of the sea [13]. In order to quantify these phenomena, experimental [8] and numerical tools [6, 7] are being developed. A three-dimensional "Particle Code", initially issuing from Pinon [9], taking into account for the non stationary evolution of the wake generated by a turbine is presented, and the comparison of experimental and numerical results is made.

The experiments were carried out in the Ifremer wave and current circulation flume tank. These experimental trials were dedicated to measure the behaviour of a tri-bladed horizontal axis turbine and to characterize the wake generated by its rotor. The behaviour of the turbine is quantified by the measurement of the thrust and the amount of power generated by the rotor, while the wake is characterized with a 2D Laser Doppler Velocimetry system.

The first tests of the method were presented in [6] and compared to results given in [2]. In order to extend this work we work on an other blade geometry: the TGL (Tidal Generation Limited [14]) commercial one.

## 2. Experimental set-up and results

The turbine used for these trials was developed by TGL before the design of a 500 kW fully submerged tidal turbine prototype, designed for deep water generation. In order to conduct our work at a representative scale and without blockage effects [4], trials were carried out on a 1/30th scale model mounted on a six-component load cells. The tri-bladed rotor was connected to a motor-gearbox assembly capable to provide active rotor speed control (gearbox, DC motor,

ballast load, motor speed control unit). The pitch of the three blades was adjustable between tests. The diameter of the tested rotor is 0.7 m, which created a blockage ratio (percentage of cross-sectional area occupied by the blades) of approximately 5 %. The model was tested at speeds ranging from 0.5 to 1.5 m/s and the turbine performances was obtained over a range of rotor speed from 10 to 190 rpm [3]. The goals of these tests are :

- to determine the effects of changing flow characteristics (homogeneous flow, flow with a velocity gradient, flow orientation, turbulence intensity) on the operational loads with a six-component load cells
- to characterise the wake of the turbine for different flow conditions (incidence, turbulence intensity, turbine location) with a 2D laser doppler velocimeter
- to measure the load on an instrumented blade with the use of strain gauges.

Velocity measurements have been performed using the 2D LDV system in the horizontal plain at the centre of the tri-bladed turbine. The velocity components were measured at twenty five probe locations in transverse direction from  $Y = -1.7$  to  $+1.7 D$  with a space step of ten centimetres. Ten locations in the wake of the turbine were considered in the range  $X = 1$  to  $10 D$  with a space step of 0.7 m.

Mean streamwise velocity distribution of a single tri-bladed horizontal axis turbine for an ambient turbulence rate of 8 % at a mid-depth location in the tank is shown in Fig. 1. It shows the extension and the decay of the wake velocity deficit. For this kind of turbine, the velocity deficit is clearly present more than 10 D downstream for a flow with a turbulence intensity of 8 %. The extension of the wake in the cross flow direction is presented on Fig. 2. The maximum decay of the wake velocity deficit is close to 60 % until 5.5 D downstream the turbine for  $TI = 8$  %. A decay of 80 % in the wake velocity deficit for water streamwise velocity is obtained (for an ambient turbulence intensity of 8 %) at 9.5 D downstream.

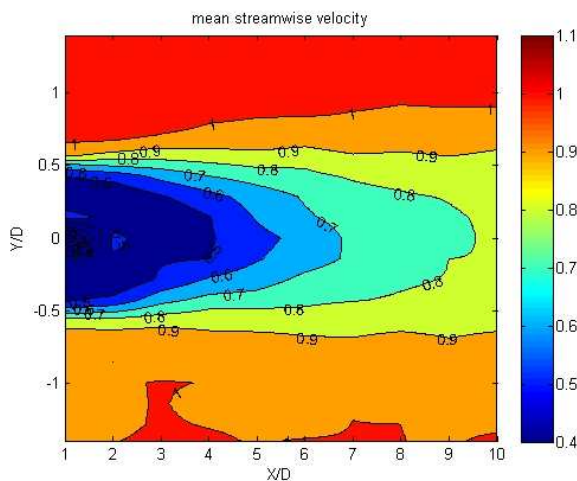


**Figure 1:** Contours of mean streamwise velocity deficit at  $TSR=5$  in the central section.

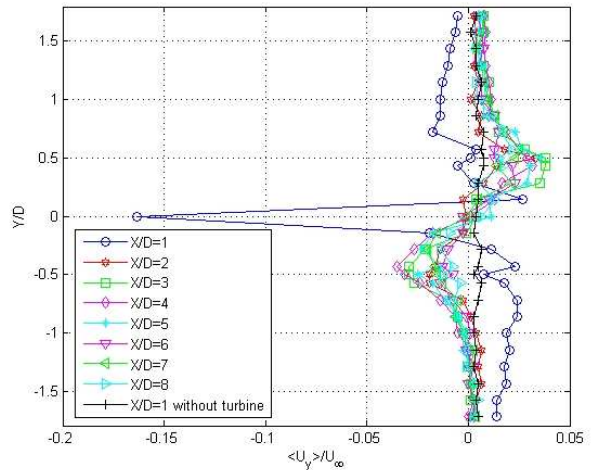


**Figure 2:** Contours of mean cross-stream velocity deficit at  $TSR=5$  in the central section.

The near wake of this turbine is more developed than for the turbine used in [8]. In the present case, the velocity deficit is 10 % higher until 5 D than for the previous one (Fig. 3), and after 6 D, the far wake reach the same level than previously.

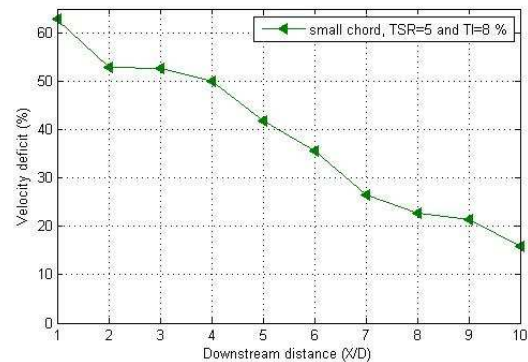


**Figure 3:** Mean centreline streamwise velocity deficit at  $TSR=5$ .

Fig. 6 shows the measured electrical power generated by holding at a specific constant rotational speed of the turbine (by dissipating power through load resistors) for an homogeneous flow an ambient turbulence intensity of 8 %. The power values given here take into account the losses in the gearbox and the inefficiencies of the motor itself. These results can be thus directly used for numerical comparisons.

### 3. Numerical modelling

In parallel with experiments, numerical predictions of performances and wake characteristics were performed with the “Particle Code”. The rotor blade geometry and flow conditions are similar than the ones used for the experiments. A short description of the numerical method is presented here knowing that the complete one is given in [7].

#### 3.1 Vortex method

The flow is discretised with particles carrying vorticity, which are advected in a Lagrangian frame. The turbine blades are taken into account thanks to a

panel method with doublet and the particles are emitted at the trailing edge of the blades using the Kutta-Joukowski condition.

The flow of an incompressible fluid is governed by the Navier-Stokes equations, which are taken here in a velocity-vorticity formulation ( $U, w$ ). The velocity is decomposed into the sum of different contributions described as the following:

$$U = U_{\infty} + U_{\phi} + U_{\omega} \quad (1)$$

with  $U_{\infty}$  the upstream velocity field,  $U_{\omega}$  the velocity field induced by the presence of the vortex particles and  $U_{\phi}$  the potential velocity field for the account of the turbine blades.

The rotational component of the velocity  $U_{\omega}$  is obtained by the Biot-Savart Law:

$$U_{\omega}(\mathbf{r}) = \frac{1}{4\pi} \int_v \mathbf{K}(\mathbf{r} - \mathbf{r}') \wedge \omega(\mathbf{r}') dv' \quad (2)$$

with  $K(r) = \frac{r}{r^3}$ . In order to avoid collapse of the

computations when two particles are getting to close, a desingularised kernel is used as in [5]:

$$\mathbf{K}_{\delta}(\mathbf{r}) = \frac{\mathbf{r}}{(\mathbf{r}^2 + \delta^2)^{3/2}} \quad (3)$$

On top of that, we developed a *Tree Code* algorithm in order to speed up the determination of the velocity  $U_{\omega}$  in eq. (2).

For the potential velocity  $U_{\phi}$ , the turbine blade surface ( $S$ ) is discretised into  $N_p$  surface elements, each surface element has a normal unit vector  $n$  and a surface  $ds$ .  $P$  is a control point located at the center of the considered surface element of the turbine blade. Assuming that the doublet contribution is constant on the surface element, the velocity component  $U_{\phi}$  is defined as in eq. (2) thanks to a matrix system [7].

$$U_{\phi} = \frac{1}{4\pi} \sum_{p=1}^{N_p} \mu_P \nabla_M \frac{\text{MP.n}(P)}{|\text{MP}|^3} ds \quad (4)$$

### 3.2 Turbine modelling

The turbine is represented by the rotor composed of three blades (Fig. 4) without hub and nacelle upon which a distribution of forces acts upon the incoming flow. The blades are considered as mean profile. The shape of the blades is one used by TGL for their first commercial turbine. The blade radius  $R$  and the free stream velocity  $U_{\infty}$  (uniform) have been set to 1. We imposed different rotational speeds  $\Omega$  in order to have

a range of tip speed ratio  $TSR = \frac{\Omega R}{U_{\infty}}$  going from 0.5

to 5. As the computations were run dimensionless, all the result will be presented non dimensional.

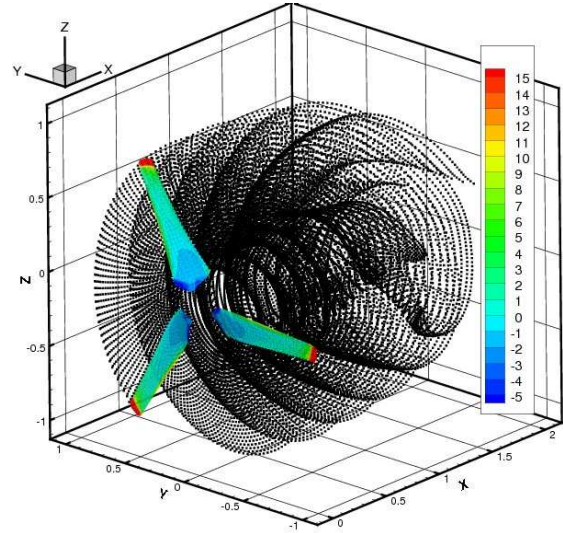


**Figure 4:** Visualisation of non dimensional total pressure on the blades and emitted particles in the near wake region.

## 4. Numerical results and comparisons

On Figure 7, one can observe the non dimensional total pressure distribution on the blades and the emitted particles in the wake for an early stage of the unsteady computation. Each blade's wake can be clearly identified. The blades are discretised into  $N_c$  elements for the chord and  $N_s$  elements for the span, so that the total number of mesh elements is defined by  $N_p = 3 \cdot N_c \cdot N_s$  as there is 3 blades on the turbine (Cf. Table 1).  $3N_s$  vortical particles emitted at each blade's trailing edge for each time step  $dt$ , which have been defined according to the tip speed ratio  $TSR$  (Cf. Table 2). The presented computations were run on a parallel architecture thanks to the MPI (Message Passing Interface) libraries, a cluster of 6 processors (Intel Xeon Quad Core duo, 2.66GHz).

$N_c \times N_s$	Matrix Size	$N_e$	$d\ell/R$
10 × 20	600 × 600	60	≈ 0.050
10 × 30	900 × 900	90	≈ 0.033
10 × 40	1,200 × 1,200	120	≈ 0.025
10 × 50	1,500 × 1,500	150	≈ 0.020

Table 1: *Geometrical description of the blades.*

The determination of the pressure has been realised thanks to a techniques presented in Rouffi [11]. Concerning the Power Coefficient:

$$C_p = \frac{Q\omega R}{\frac{1}{2} \rho \pi R^2 U^3},$$

the first thing was to determine

$Q$  the rotational speed torque. Figure 5 presents the evolution of the rotational speed torque  $Q$  as time evolves for different  $TSR$ . After an initialisation phase ( $0.0 < t < 3.0$ ),  $Q$  tends to a constant value, clearly obtains for each simulation case for  $t > 4.0$ , except for

the larger  $TSR$  (ie  $TSR > 4.5$ ). In order to determine the  $C_p$ , we determined the mean value and the standard deviation of  $Q$  for time comprised in  $4.0 < t < 6.0$ .

$TSR$	$\Omega \times R$	$dt$	$N_{iter}$
0.5	1,118	0,036	168
1.0	1,414	0,028	212
1.5	1,803	0,022	270
2.0	2,236	0,018	335
2.5	2,693	0,015	404
3.0	3,162	0,013	474
3.5	3,640	0,011	546
4.0	4,123	0,010	618
4.5	4,610	0,009	691
5.0	5,099	0,008	765

Table 2: Description of the time step depending on the  $TSR$ .

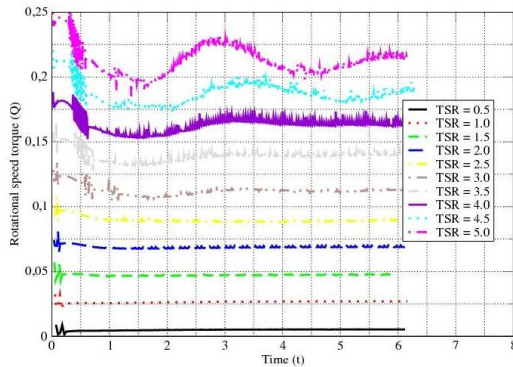


Figure 5: Rotational speed torque as a function of time for different  $TSR$  for a TGL computation with a discretisation of  $10 \times 30$  and parameters defined as in Table 2.

Figure 6 describes the evolution of  $C_p$  for different discretisations of the blades. For the moment, only a variation of  $N_s$ , the number of elements onto the span, has been evaluated. Variation of  $N_c$ , the number of elements onto the chord, will be realised shortly.

Nevertheless, from Fig. 6 one can observe that, beyond the discretisation  $10 \times 30$ , the  $C_p$  values do not change and we are converged concerning the Power Coefficient with respect to  $N_s$  discretisation. A comparison of these results has been realised with the experimental results described previously. One can observe that we are in fairly good coherence with a slight tendency of underestimation except, once more, for the larger  $TSR$ . The explanation of the general underestimation are twofold : first, the convergence study has not been completed yet (chord discretisation  $N_c$  and regularisation parameter convergence). The second, but probably not least in terms of importance, is that the so-called wing tip vortices or blade tip vortices generated at each blade tip is not treated in the present study. Previous tests, not presented here, have shown these vortices could have a non-negligible influence on  $Q$ . For larger  $TSR$ , the overestimation tendency is mainly due to the fact that

flow detachment on the blade cannot be considered here whatever the incident flow is. The issue has been discussed in [6]; an enhancement of the emission scheme will be realised in short term in that purpose.

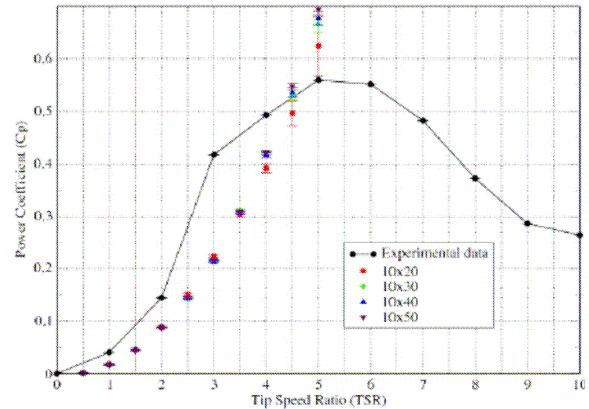
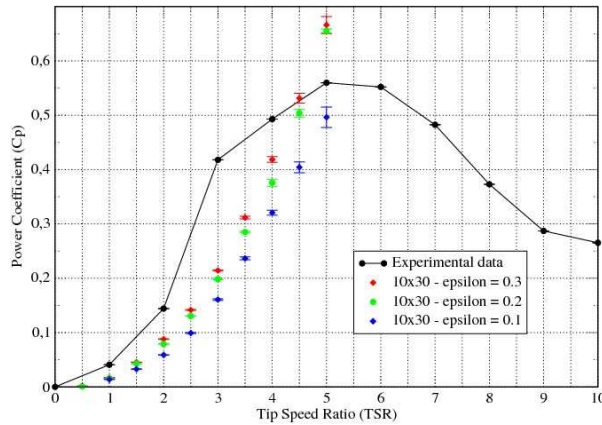


Figure 6: Power coefficient as a function of  $TSR$  for different discretisation of the blades.

Figure 7 describe the numerical converge with respect to the regularisation parameter for a fix blade discretisation (i:e  $10 \times 30$ ). One can observe that the smaller regularisation is, the larger the general underestimation is. Two conclusions can be drawn from these results : first, no convergence in term of  $C_p$  has been achieved yet and smaller regularisation need to be tested and evaluated. The second conclusion would be that smaller regularisation will probably emphasize the general underestimation. However, smaller regularisation parameters lead to a smaller flow discretisation in term of particles interspacing. This lead to a better description of the flow structures, and also a better account of the blade tip vortices when they will be treated. However, smaller regularisation will increase the total number of particles in the flow that will automatically increase CPU time consumption. To conclude with that aspect, the account of blade tip vortices and flow detachment onto the blade are now necessary to enhance the quality of the present results. Better discretisation will also improve the results quality together with an increase of CPU time consumption.

Concerning velocity profiles in the turbine wake, first attempts have been realised in [6] with promising results. Since then, a few implementation in the numerical tool have been performed. But, in order to have the complete evolution of the wake, huge computations will be required. In fact, having a look at Table 3, one can see that an *ideal* particle inter-spacing distance would be  $dl/R = 0.03333$  for the blade discretisation  $10 \times 30$  (See Table 1). This *ideal* particle inter-spacing distance corresponds to a regularisation parameter of  $0.05 = 1.5 dl$ . So the total number of particles for this computation has been evaluated around 3,400,000 if we suppose that the wake develops upon 10 diameters without spreading too much in the radial distance (which is a strong hypothesis). On top of that, more than thousands unsteady times steps  $dt$

would be required in order to be in a quasi-steady state of the wake. These types of computations require large amount of CPU resources, and we are currently working on that.



**Figure 7:** Power coefficient as a function of *TSR* for a 10 x 30 different discretisation of the blades and different regularisation parameters.

$\delta/R$	$dl/R$	$dv = dl^3$	$N_\omega$
0.3000	0.20000	0.008000	$\approx 16,000$
0.2000	0.13333	0.002370	$\approx 53,000$
0.1000	0.06666	0.000296	$\approx 420,000$
0.0500	0.03333	0.000037	$\approx 3,400,000$

Table 3: *Particles discretisation of the flow (i.e particle inter-spacing  $dl$ ) and the evaluated total number of particles  $N_\omega$  at the end of the computation.*

## 5. Conclusion

These preliminary comparisons show that the numerical results are in good agreement with the experimental one, especially in terms of power. An increase of the computation duration, the number of mesh elements and the number of particles will improve the development of this numerical code is still in progress. The free surface, boundary layer velocity profile and an unsteady fluctuation of this profile will be implemented step by step in order to take into account for the global environment of marine current turbines. The first results given here will be extended in the near future. These numerical tools could be used prior to the installation of a marine current turbine farm, with the aim to examine and assess its potential environmental impact. Understanding the effect these devices have on the flow is also critical in determining how one device may modify both the performance of and loading experienced by another device in an array.

## Acknowledgements

The authors wish to thank the Région Haute-Normandie for the financial support (co-financing of the PhD) of this collaborative work with TGL carried out in the Ifremer flume tank. We also would like to acknowledge and thank the following people for their implication in the project: J. King, J.V. Facq and B. Gaurier.

## References

- [1] A.S. Bahaj and L. Myers. Analytical estimates of the energy yield potential from the Alderney Race (Channel Islands) using marine current energy converters. *Renewable Energy*, 29 : 1931-1945, 2004.
- [2] A.S. Bahaj, W.M.J Batten and G. Mc Cann. Experimental verifications of numerical predictions for hydrodynamic performance of horizontal axis marine current turbines. *Renewable Energy*, 32 : 2479-2490, 2007.
- [3] G. Germain, A.S. Bahaj, P. Roberts, C. Huxley-Reynard. Facilities for marine current energy converter characterization. 7<sup>th</sup> EWETEC, Porto, September 2007.
- [4] G. Germain. Marine current energy converter tank testing practices. ICOE 2008, Brest.
- [5] K. Lindsay and R. Krasny. A particle method and adaptive treecode for vortex sheet motion in three-dimensional flow. *J. Comput. Phys.* Vol 172, 2001.
- [6] F. Maganga, G. Pinon, G. Germain and E. Rivoalen. Numerical simulation of the wake of marine current turbines with a particle method. WRECX 2008, Glasgow.
- [7] F. Maganga, G. Pinon, G. Germain and E. Rivoalen. Numerical and experimental characterizations of uid/structure interaction effects generated by marine current turbines farm in its environment. ICOE 2008, Brest.
- [8] F. Maganga, G. Germain, J. King, G. Pinon and E. Rivoalen. Flow characteristic effects on marine current turbine behaviour and on its wake properties. IET Renewable Power Generation, under revision.
- [9] G. Pinon, H. Bratec, S. Huberson, G. Pignot and E. Rivoalen. Vortex method for the simulation of a 3D round jet in a cross-stream. *J. Turbulence*, Vol. 6 N18, 2005.
- [10] L. Rosenhead. The formation of vortices from a surface of discontinuity. *Proc. Soc. London*, A(134): 170-192, 1931.
- [11] F. Rouffi. Résolution numérique de problèmes non linéaires de l'hydrodynamique navale : manoeuvrabilité et tenue à la mer des navires. PhD thesis, Université Pierre et Marie Curie, 1992.
- [12] M. A. Shields, L. J. Dillon, D.K. Woolf and A. T. Ford. Strategic priorities for assessing ecological impacts of marine renewable energy devices in the Pentland Firth (Scotland, UK). *Marine Policy*, 2008.
- [13] X. Sun, J. P. Chick and I. G. Bryden. Laboratory-scale simulation of energy extraction from tidal currents. *Renewable Energy*, 33 : 1267-1274, 2008.
- [14] <http://www.tidalgeneration.co.uk/>